ELSEVIER

FEMS Microbiology Ecology 34 (2001) 197–206

FEMS MICROBIOLOGY Ecology

www.fems-microbiology.org

A new look at microbial leaching patterns on sulfide minerals

Katrina J. Edwards [a,*], Bo Hu [b], Robert J. Hamers [b], Jillian F. Banfield [a]

[a] *Department of Geology and Geophysics, University of Wisconsin-Madison, 1215 West Dayton Street, Madison, WI 53706, USA*
[b] *Department of Chemistry, University of Wisconsin-Madison, 1101 University Ave., Madison, WI 53706, USA*

Received 26 May 2000; received in revised form 16 September 2000; accepted 19 September 2000

Abstract

Leaching patterns on sulfide minerals were investigated by high-resolution scanning electron microscopy (SEM). Our goal was to evaluate the relative contributions of inorganic surface reactions and reactions localized by attached cells to surface morphology evolution. Experiments utilized pyrite (FeS_2), marcasite (FeS_2) and arsenopyrite (FeAsS), and two iron-oxidizing prokaryotes in order to determine the importance of cell type, crystal structure, and mineral dissolution rate in microbially induced pit formation. Pyrite surfaces were reacted with the iron-oxidizing bacterium *Acidithiobacillus ferrooxidans* (at 25°C), the iron-oxidizing archaeon '*Ferroplasma acidarmanus*' (at 37°C), and abiotically in the presence of Fe^{3+} ions. In all three experiments, discrete bacillus-sized (1–2 μm) and -shaped (elliptical) pits developed on pyrite surfaces within 1 week of reaction. Results show that attaching cells are not necessary for pit formation on pyrite. Marcasite and arsenopyrite surfaces were reacted with *A. ferrooxidans* (at 25°C) and '*F. acidarmanus*' (at 37°C). Cell-sized and cell-shaped dissolution pits were not observed on marcasite or arsenopyrite at any point during reaction with *A. ferrooxidans*, or on marcasite surfaces reacted with '*F. acidarmanus*'. However, individual '*F. acidarmanus*' cells were found within individual shallow (< 0.5 μm deep) pits. The size and shape (round rather than elliptical) of the pits conformed closely to the shape of *F. acidarmanus* (cells) pits on arsenopyrite. We infer these pits to be cell-induced. We attribute the formation of pits readily detectable (by SEM) to the higher reactivity of arsenopyrite compared to pyrite and marcasite under the conditions the experiment was conducted. These pits contributed little to the overall surface topographical evolution, and most likely did not significantly increase surface area during reaction. Our results suggest that overall sulfide mineral dissolution may be dominated by surface reactions with Fe^{3+} rather than by reactions at the cell–mineral interface.

Keywords: Pyrite; Marcasite; Arsenopyrite; Surface reaction; Microbial attachment; Dissolution; *Acidithiobacillus ferrooxidans*; *Thiobacillus ferrooxidans*; '*Ferroplasma acidarmanus*'

1. Introduction

The kinetics and mechanisms of microbial oxidation of sulfide minerals, mainly pyrite, have been the focus of considerable attention due to the economic importance of bioleaching, and the environmental damage associated with alteration of pyrite-rich ore (acid mine drainage; AMD). Studies of pyrite oxidation have most commonly been conducted with the iron-oxidizing acidophile, *Acidithiobacillus ferrooxidans* (formerly known as *Thiobacillus ferrooxidans* [1]). *A. ferrooxidans* is found in drainage waters associated with many AMD environments and is known to accelerate the rate of pyrite oxidation [2].

Interactions between attached iron-oxidizing cells and sulfide surfaces are believed to play a crucial role in oxidative dissolution. Specifically, attached cells are believed to either 'directly' or 'indirectly' control surface oxidation reactions. In either case, reactions that occur between the cells and the mineral surface are thought to result in characteristic leaching patterns that form on pyrite [3]. The term 'direct' was introduced by Silverman and Ehrlich in 1964 [4] to describe a hypothesized enzymatic reaction taking place between an attached cell and the underlying mineral surface. The 'indirect' mechanism of sulfide oxidation involves non-specific oxidation of surfaces by Fe^{3+} that is generated by iron-oxidizing microorganisms.

Local enhanced dissolution in proximity to attached cells could occur, even if sulfide oxidation occurs via a direct or indirect mechanism. However, in the case of the indirect pathway, local increase in reactivity is only expected if reaction rates between Fe^{3+} and surface sulfide

* Corresponding author. Present address: Woods Hole Oceanographic Institution, Department of Marine Chemistry and Geochemistry, McLean Lab, Mail Stop 8, Woods Hole, MA 02543, USA. Tel.: +1 (508) 289-3620; Fax: +1 (508) 457-2183;
E-mail: kedwards@whoi.edu

0168-6496/01/$20.00
PII: S0168-6496(00)00094-5

groups are fast compared to rates of diffusion of Fe^{3+} away from the cell surface. Thus, microbially induced pit formation may depend upon the reactivity of the sulfide phase as well as the presence of potential diffusion inhibiting factors, such as polymers, around cells.

In 1978, two separate papers reported similar observations of *A. ferrooxidans* on sulfide mineral surfaces [5,6] that seemed to support the existence of the direct mechanism. Both groups described pitting patterns, the size and shape of which were interpreted to be the result of reactions that occurred at cell–mineral interfaces. Several workers since this time have reported similar findings [7,8]. The inference of direct interaction between iron-oxidizing cells and the surfaces they are attached to is supported by studies that have shown that *A. ferrooxidans* does not develop into multilayer biofilms on pyrite surfaces [9]. These observations are thought to imply that each cell needs to be in direct contact with the pyrite surface in order to grow [10]. In addition, it has been found that *A. ferrooxidans* is able to distinguish and selectively colonize minerals that are more reactive, implying that close contact between the cells and the sulfide substrate is important for solubilization [11].

Several models have been developed to describe the reactions that take place between cells and mineral surfaces that result in the pitting patterns that have been observed [8,9,12]. Rodriguez et al. [8] proposed that *A. ferrooxidans* formed a 'pseudo capsule' around the leaching region that facilitates increased rates of reaction around the cell, causing it to 'burrow' into the sulfide surface. Sand et al. [9] proposed that *A. ferrooxidans* and probably '*Leptospirillum ferrooxidans*' (another common iron-oxidizing acidophile) utilize ferric iron compounds contained within their exopolymer layers to facilitate enhanced reaction at the cell–mineral interface, ultimately producing the pits that are observed. Sand et al. [9], however, claim that iron compounds within the extracellular polymer layers of *A. ferrooxidans* catalyze oxidative dissolution; hence, the reaction results from an indirect, or non-enzymatic mechanism.

Here we report findings from a low-voltage, field emission scanning electron microscopy (SEM) study on microbial leaching patterns on pyrite, marcasite, and arsenopyrite using *A. ferrooxidans* and an iron-oxidizing archaeon, *Ferroplasma acidarmanus*. Our results for *A. ferrooxidans* suggest that pitting patterns on pyrite are intrinsic to this mineral, hence, may not always arise from specific cell–mineral interactions. However, results from experiments with *F. acidarmanus* indicate that detectable pits develop at the cell–mineral interface when cells are attached to more reactive phases such as arsenopyrite. Despite the enhanced etching in proximity to cells, the interaction of surfaces with Fe^{3+} appears to play a larger role in overall surface topographical evolution, and hence overall reaction. Pitting patterns that develop on microbially reacted pyrite surfaces are compared with pitting patterns on pyrite reacted abiotically with Fe^{3+}. Implications for reaction mechanisms and modeling of bioleaching are discussed.

2. Materials and methods

2.1. Strains and growth conditions

ATCC 19859 was used for experiments with *A. ferrooxidans*. The archaeal species *F. acidarmanus* [13] was used for comparative experiments. *F. acidarmanus* is a mixotrophic iron-oxidizing archaeon within the Thermoplasmales family, closely related to the autotrophic iron-oxidizing species *Ferroplasma acidophilum* [14].

Cells were cultured in media salts that have been described elsewhere [15], with 20 g l^{-1} $FeSO_4$ for the energy source, adjusted to pH 2.5 for *A. ferrooxidans*, and 1.5 for *F. acidarmanus* with H_2SO_4. The medium for *F. acidarmanus* was supplemented with 0.002% yeast extract. *A. ferrooxidans* cells were grown at 25°C under aerated conditions. *F. acidarmanus* was grown at 37°C unshaken.

2.2. Minerals

All sulfide minerals used here were purchased from Wards Scientific. Pyrite (FeS_2; Spain) and marcasite (FeS_2; Indiana) samples were both of diagenetic origin. Single whole crystals (pyrite) or massive aggregates (arsenopyrite, FeAsS, and marcasite) were used to prepare thin polished slabs used for microscopy, and for supplemental crushed material. The preparation of polished pyrite blocks and crushed material is described in detail elsewhere [16]. Briefly, blocks ($\sim 1 \times 3 \times 3$ mm) of each mineral with one polished face were prepared using a method similar to that used to make normal, petrographic thin sections. Three–6 blocks were used per experiment. Blocks were supplemented with approximately 2 g of cleaned (rinsed with distilled water and treated with 10% HCl for 2 h), crushed material (150–500 μm diameter). In order to avoid oxidation of surfaces (during autoclaving) that were intended for microscopic analysis, blocks were sterilized by soaking in 100% ethanol for 2 h prior to experiments. Controls verified the sterility of the experimental materials following this procedure. Crushed material and flasks were autoclaved at 126°C and 20 psi for 20 min prior to the addition of blocks.

2.3. Experimental procedures

Cells that were grown on the above described medium for 1 week were harvested by centrifugation and washed once in distilled water adjusted to pH 1.5 with sulfuric acid. Cells were resuspended in medium salts (without ferrous sulfate), pH 2.3 (*A. ferrooxidans*) or pH 1.5 (*F. acidarmanus*). Two ml of cell suspension was inoculated into (250 ml) flasks containing the minerals (crushed material

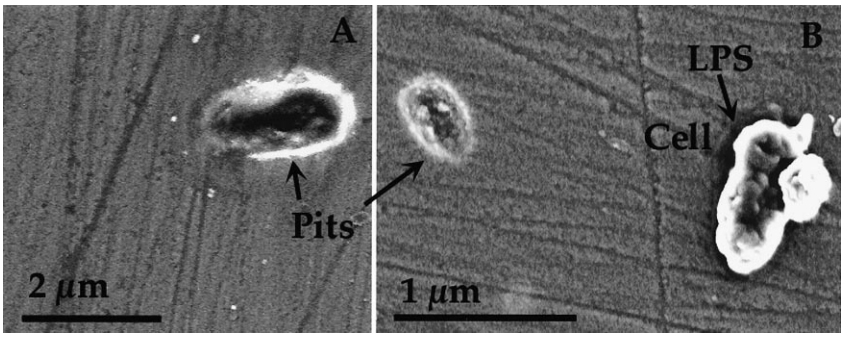

Fig. 1. SEM image of a typical example of pit formation and an *A. ferrooxidans* cell at the early stages (1 week of reaction) of pyrite dissolution. Dissolution pits that are approximately cell-sized and bacillus-shaped are frequently found (A, B), but *A. ferrooxidans* cells are not found within them (B). Note presence of what we infer is dehydrated polysaccharide material (LPS; [17]) exterior to the cell wall.

and blocks) and 35 ml of medium. Flasks with *A. ferrooxidans* and corresponding controls (no inoculum) were incubated unshaken at 25°C for 4 weeks. Flasks with *F. acidarmanus* and corresponding controls (no inoculum) were incubated unshaken at 37°C for 22 days.

Blocks were taken from the flasks on a weekly basis with autoclaved forceps. Pyrite blocks reacted with *A. ferrooxidans* during the first 2 weeks were rinsed thoroughly with distilled water and air-dried after removing from flasks. The remainder of the blocks (pyrite and all marcasite and arsenopyrite samples) were soaked in acidified distilled water (adjusted to pH 1.5 with H_2SO_4) for approximately 1 min, then rinsed in the same acidified water. This was done in order to remove surface precipitates that were observed to accumulate, partially obscuring the cells (see below).

F. acidarmanus cells readily lyse and require fixation for intact cell preservation. Hence, blocks reacted with *F. acidarmanus* were taken from flasks with autoclaved forceps and fixed in 4% paraformaldehyde in 1×phosphate-buffered saline solution (0.137 M NaCl, 0.005 M $NaHPO_4{\cdot}7H_2O$, 0.003 M KCl, 0.001 M KH_2PO_4), pH 7.3 for 2 h. Blocks were then rinsed thoroughly with ethanol and distilled water.

Experimental methods used for ferric iron dissolution experiments are described elsewhere by Hu et al. (in preparation), who have characterized the surface chemistry, microstructural evolution, and surface spectroscopy of pyrite reacted with ferric iron. Pyrite blocks (prepared similar to the above procedure) were reacted in Teflon vessels in 0.01 M ferric sulfate solution, adjusted to pH 1.5 with sulfuric acid. Experiments were run at 42°C. Blocks were taken out at 3.7, 12.5, and 28.5 days for analysis. Samples were rinsed twice with distilled water and air-dried.

Microbially reacted mineral blocks and controls were carbon-coated for electron microscopy. Abiotically reacted samples (Fe^{3+}-reacted samples and control samples) were examined uncoated. SEM analysis of blocks was done using a LEO DSM-982 Field Emission SEM (FE SEM) microscope (operated at 3 kV). Six–12 colonized (by *F. acidarmanus* or *A. ferrooxidans*) sections of each mineral specimen were imaged. Representative images were selected for use as figures in this paper. Tens of images of *F. acidarmanus* and *A. ferrooxidans* cells attached to each mineral specimen were examined at high magnification (>10 000×).

3. Results

3.1. A. ferrooxidans on pyrite

Fig. 1 shows a typical example of a pyrite surface at the early stages of dissolution (1 week). Shallow, approximately cell-sized (1–2×0.5–1 μm) and bacillus-shaped pits were observed (Fig. 1A,B). *A. ferrooxidans* cells were found in the vicinity of these shallow, cell-sized dissolution pits (Fig. 1B), however, were not observed within detectable cell-sized and -shaped dissolution pits.

Average pit size and pitting density on the surfaces increased with reaction time. After 4 weeks, surface pitting was extensive, resulting in discrete, euhedral, and sometimes elongate pits up to 80 μm in length (Fig. 2).

Many cells showed extensive polymer development by

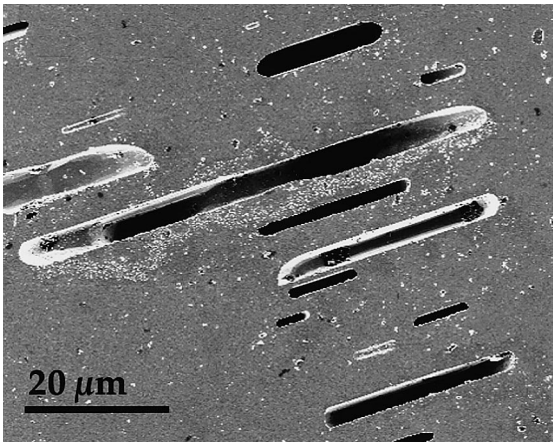

Fig. 2. SEM image of pit development on a pyrite surface after 4 weeks of reaction at 25°C with *A. ferrooxidans*.

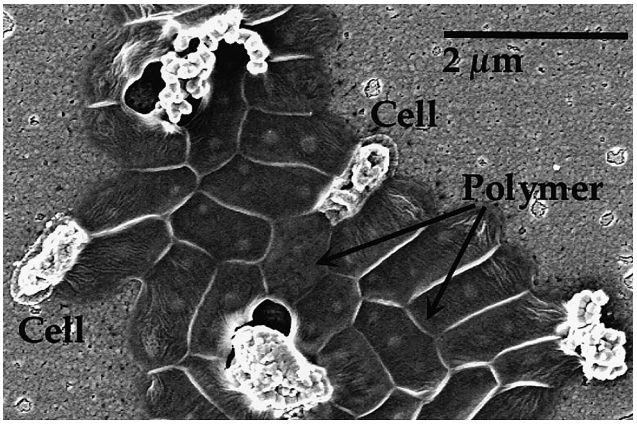

Fig. 3. SEM image of five *A. ferrooxidans* cells (partially to completely covered by mineral precipitates) attached to a pyrite surface and surrounded by extracellular polymer. Surfaces were reacted for 14 days (at 25°C).

2 weeks and were covered by secondary mineral deposits, likely ferric iron precipitates that are commonly associated with *A. ferrooxidans* [17]. Fig. 3 shows *A. ferrooxidans* cells on a pyrite surface surrounded by extracellular polymer that exceeds that amount of surface covered by the cells almost an order of magnitude (note though that these are subject to dehydration artifacts).

Mineral deposits were localized at cell walls and at edges of the lipopolysaccharide (LPS) and extracellular polymers. Fig. 4 shows mineral deposits that have formed at the edges of the LPS (Fig. 4A), and extracellular polymer (Fig. 4B). *A. ferrooxidans* cells were also found encased in mineral deposits. Fig. 5 shows a cell that is extensively covered in mineral deposits (Fig. 5A), and what may be the mineral husk of a lysed cell (Fig. 5B). At no

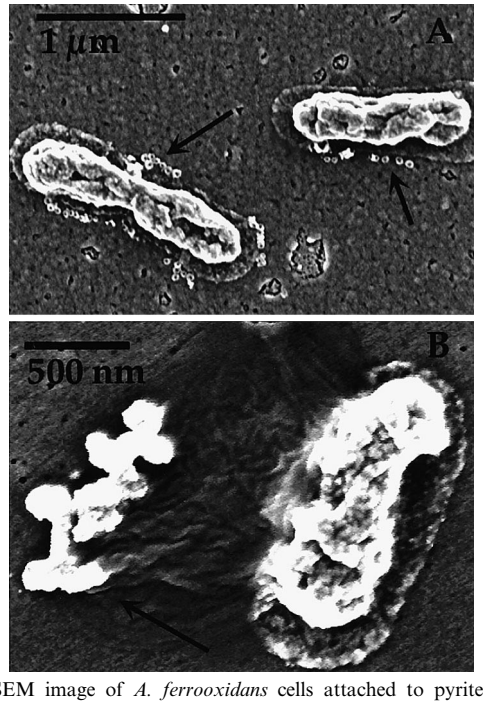

Fig. 4. SEM image of *A. ferrooxidans* cells attached to pyrite surfaces and surrounded by polymer. Mineralization of polymer is frequently found at edges of what is likely dehydrated LPS ([17]; A) and at the edges of extracellular polymer material (B). Surfaces were reacted for 14 days (at 25°C).

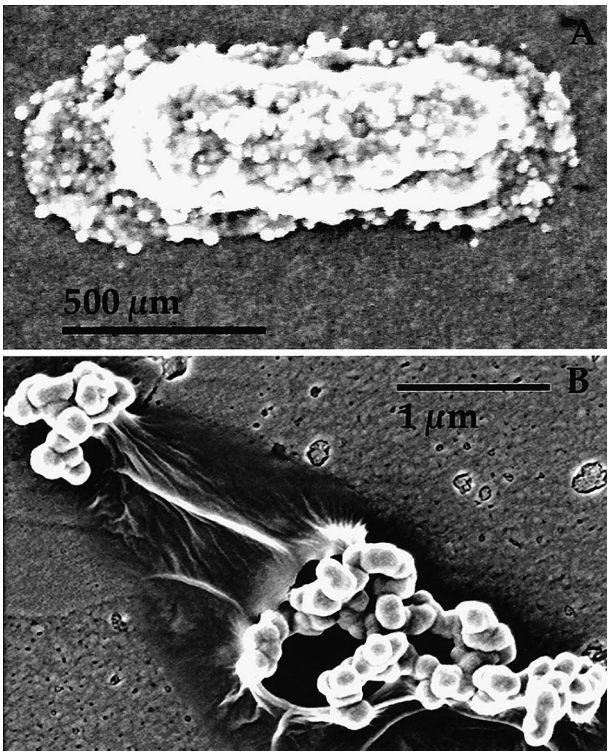

Fig. 5. (A) SEM image of an *A. ferrooxidans* cell attached to a pyrite surface that is covered extensively with mineral deposits. (B) SEM image of mineral deposits (associated with extracellular polymer) that are inferred to be the husk of a lysed cell. Deposits such as these were not ever observed on samples reacted abiotically with Fe^{3+}, nor abiotic control surfaces. Surfaces were reacted for 14 days (at 25°C).

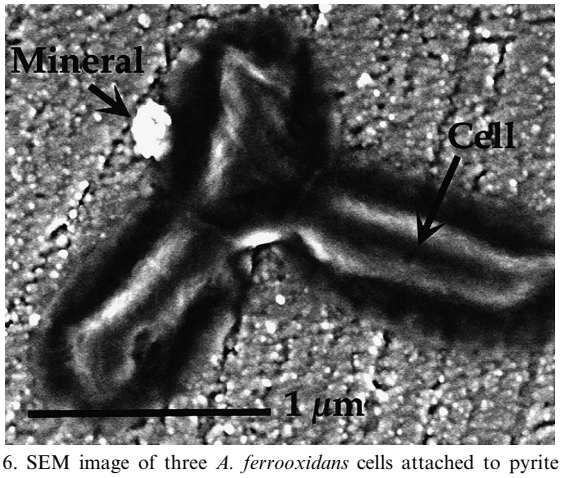

Fig. 6. SEM image of three *A. ferrooxidans* cells attached to pyrite surfaces (reacted for 28 days at 25°C) that have been acid-treated to remove mineral deposits (see Section 2). Note small residual mineral deposit. No evidence for pit formation at the edges or in the near vicinity of these cells, or any other cells observed, was detected.

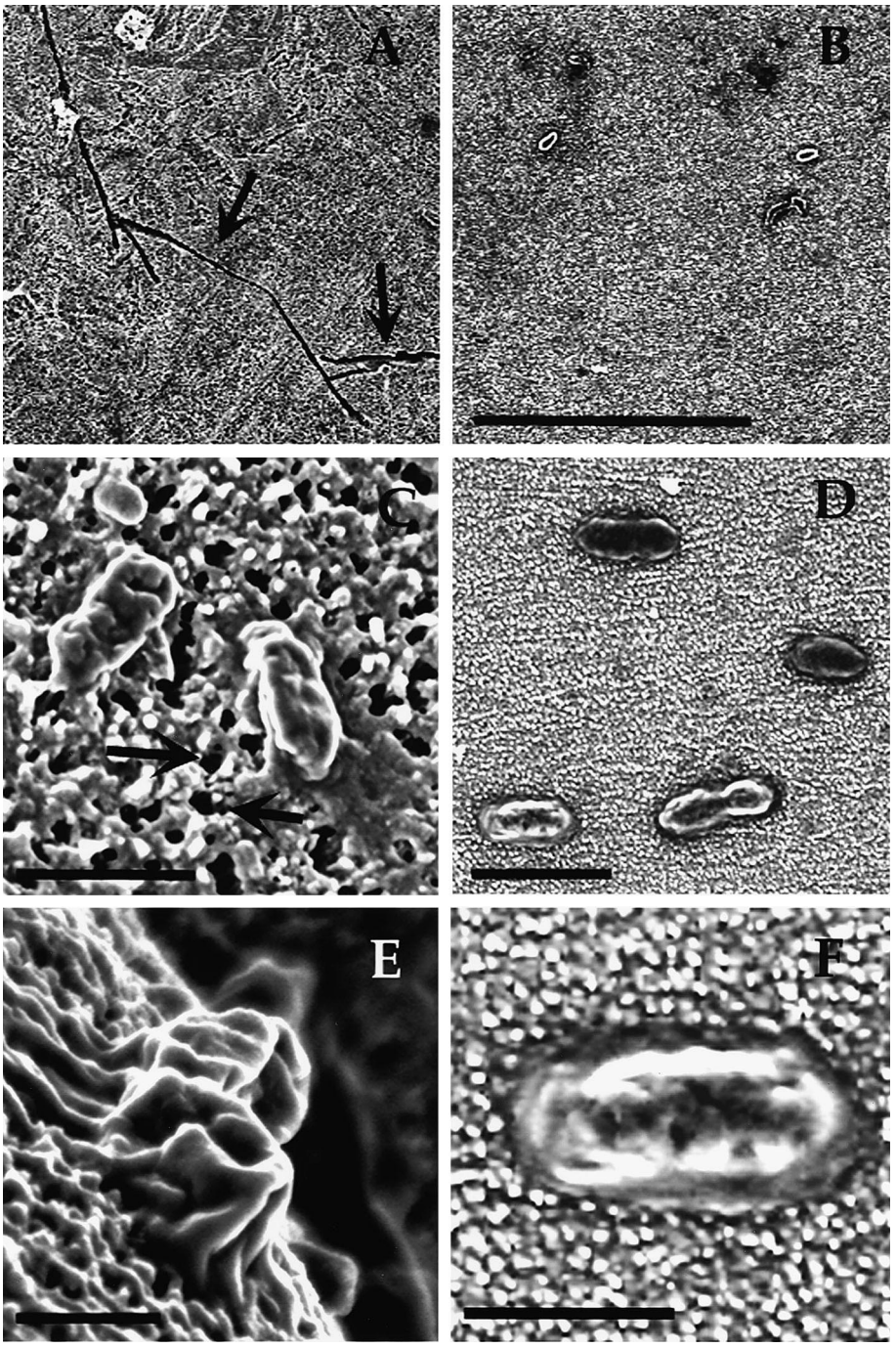

Fig. 7. SEM images of arsenopyrite (A, C, E) and marcasite (B, D, F) surfaces reacted with *A. ferrooxidans* for 22 days (at 25°C). A and B show the character of surface roughening (scale bar in B is 20 μm and applies to A). The linear dissolution features that can be seen in A (shown with arrows) appear as cracks, and were observed on marcasite as well (not shown). Small cell-sized and -shaped pits such as shown in Fig. 1, and enlarged pits of the shape shown in Fig. 2 for pyrite, were not ever observed on marcasite or arsenopyrite. C (scale bar = 1 μm) shows numerous very small, porous pits. D (scale bar = 2 μm) and F show roughened marcasite surfaces with cells of *A. ferrooxidans* attached, with no clear evidence of pit formation at the edges of, or in the vicinity of the attached cells. E (scale bar = 1 μm) shows a view on the edge of a dehydrated *A. ferrooxidans* cell attached to the roughened arsenopyrite surface, such as is shown from the top in C (e.g. upper left cell). No clear depressions are evident at the edges of the cell–mineral interface.

stage of mineral development were cells found within discernible dissolution pits such as shown in Fig. 1.

Because surface coverage by polymer and mineral precipitates may have obscured edges of shallow pits, acid treatment was employed to remove precipitates from the mineral samples and cells reacted for 3 and 4 weeks (see Section 2). After removing the precipitates from cells (Fig. 6), cells were not ever found within cell-sized and -shaped pits, nor could any other clear evidence for pit formation at the cell–mineral interface be detected by SEM.

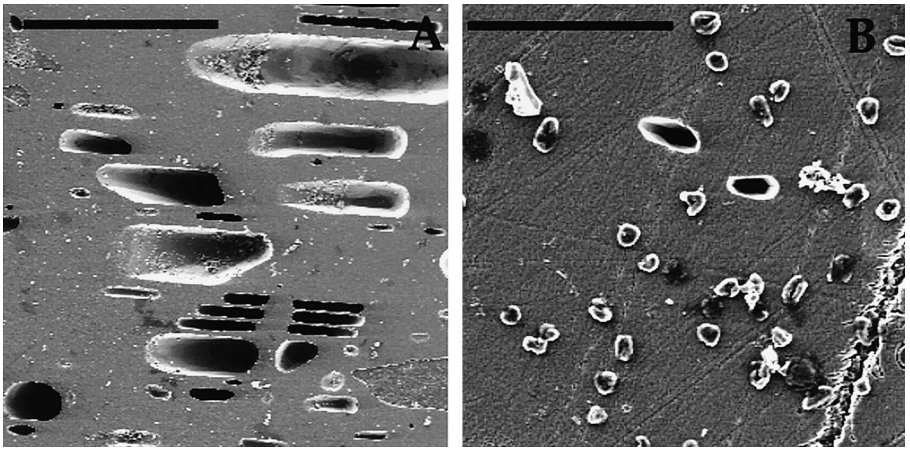

Fig. 8. SEM images of pyrite surfaces reacted with *F. acidarmanus* (at 37°C) for 14 (A) or 22 days (B). A shows elongate, well-developed dissolution pits, similar to those observed in Fig. 2 (scale bar = 50 μm). B (scale bar = 5 μm) shows *F. acidarmanus* cells on a pyrite surface, in the vicinity of, but not within, bacillus-sized and -shaped dissolution pits, similar to those shown in Fig. 1. Note cell shape of *F. acidarmanus* is roughly spherical. No cells were observed within cell-sized and -shaped pits on pyrite.

3.2. *A. ferrooxidans* on marcasite and arsenopyrite

Marcasite and arsenopyrite surfaces evolved differently from pyrite surfaces. Most notable, cell-sized or cell-shaped dissolution pits were not ever observed on marcasite or arsenopyrite. At later stages of reaction (3–4 weeks), surfaces of marcasite and arsenopyrite were more homogeneously etched (Fig. 7A,B) relative to pyrite surfaces at the same stage of reaction (Fig. 2). Some linear dissolution features (appear as deep cracks) developed on marcasite and arsenopyrite (e.g. Fig. 7A). Arsenopyrite developed a porous surface texture at later stages of reaction, with 'pores' on the order of 0.1 μm in diameter (Fig. 7C). *A. ferrooxidans* cells were not found within any cell-shaped dissolution pits, or within shallow depressions (Fig. 7E,F).

3.3. *F. acidarmanus* on pyrite, marcasite, and arsenopyrite

In general, the major surface topographical features of pyrite, marcasite, and arsenopyrite reacted with *F. acidarmanus* were very similar to the samples reacted with *A. ferrooxidans*. Fig. 8A shows large, euhedral and elongate dissolution pits that developed during reaction with *F. acidarmanus*. Fig. 8B shows cells on a pyrite surface, with small cell-sized and bacillus-shaped dissolution pits in the vicinity of the cell attachment sites, similar to what was shown in Fig. 1 for *A. ferrooxidans*. No cells were observed within cell-sized and -shaped pits on pyrite.

Marcasite surfaces did not develop discrete, cell-sized and -shaped pits when reacted with *F. acidarmanus*. Fig. 9A shows the roughened surface of marcasite with linear dissolution pits, similar to the linear dissolution features that were observed on marcasite reacted with *A. ferrooxidans*. Fig. 9B shows *F. acidarmanus* cells on a marcasite surface with no discernible pitting around the cells.

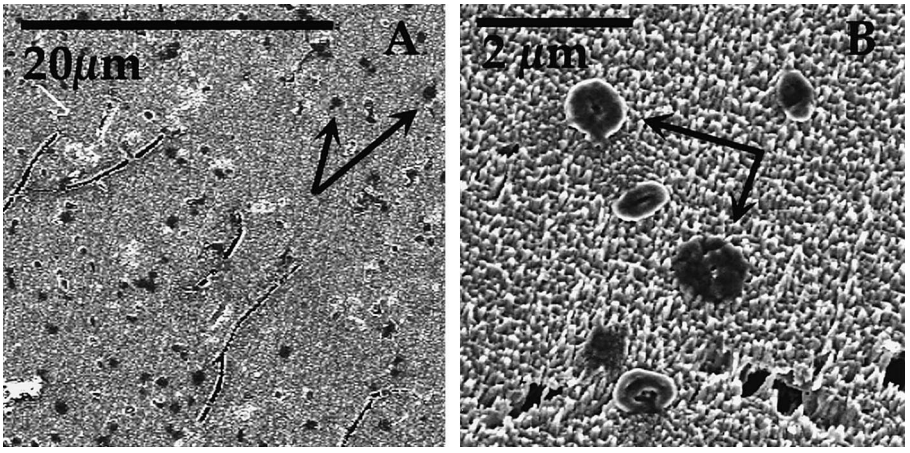

Fig. 9. SEM images of marcasite surfaces reacted with *F. acidarmanus*. Both surfaces were reacted for 22 days (at 37°C). A shows the linear dissolution features that are characteristic of marcasite dissolution. B shows higher resolution surface features and *F. acidarmanus* cells attached to the surface, with no evidence of pit formation in surrounding cells. Note similarities in surface feature between these images and those shown in Fig. 7.

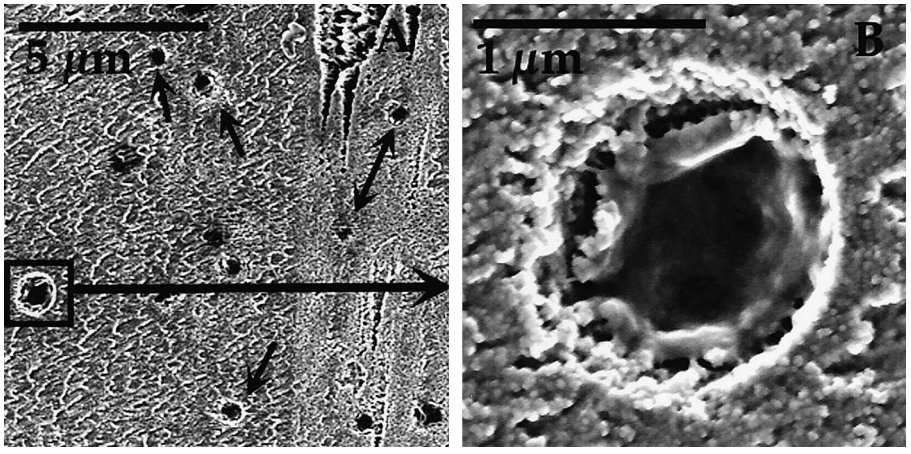

Fig. 10. SEM images of an arsenopyrite surface reacted with *F. acidarmanus* for 22 days (at 37°C). B shows high magnification of the area shown within the square in A. The dehydrated cell shown in B is clearly situated within a cell-sized and cell-shaped dissolution pit. Many other cells seen here are also within shallow, cell-sized and -shaped dissolution pits; examples are indicated with arrows in A.

Overall, arsenopyrite surfaces reacted with *F. acidarmanus* were similar to arsenopyrite surfaces reacted with *A. ferrooxidans*. Surfaces were etched fairly homogeneously, with linear dissolution features developing at later stages of reaction (Fig. 10A). However, in contrast to all other surfaces examined in this study, cell-sized and -shaped (spherical, conforming to the coccoid cell shape of *F. acidarmanus*) pits were observed between *F. acidarmanus* cells and the arsenopyrite surfaces they were attached to (Fig. 10B). Most *F. acidarmanus* cells observed on arsenopyrite after 3 weeks of reaction were situated within cell-sized and cell-shaped dissolution pits (Fig. 10A). Dissolution pits of the type seen on pyrite (bacillus cell-sized and -shaped; e.g. Figs. 1 and 8B) were not ever observed on arsenopyrite.

3.4. Abiotic control surfaces

For comparison with the microbial experiments, Fig. 11 shows examples of pyrite (Fig. 11A), marcasite (Fig. 11B), and arsenopyrite (Fig. 11C) after abiotic reaction at 37°C in medium for 22 days (abiotic control surfaces). Few discrete pits had developed on pyrite, and those observed were < 0.5 μm in maximum diameter (Fig. 11A). Marcasite and arsenopyrite surfaces etched in a similar manner (similar etching features) as the microbially reacted surfaces, though surfaces appeared less roughened. No discrete pits such as developed at the attachment sites of *F. acidarmanus* were observed on arsenopyrite. Results for surfaces reacted abiotically in medium alone at 25°C were similar to those reacted abiotically, but surface roughening (all minerals) and pitting (pyrite) occurred to a lesser degree on all minerals (not shown).

3.5. Pyrite reacted with Fe^{3+}

Fig. 12 shows examples of pyrite surfaces reacted abiotically with Fe^{3+}. Pyrite surfaces reacted abiotically with ferric iron displayed many features similar to pyrite surfaces reacted with *A. ferrooxidans* and *F. acidarmanus*. After 3.7 days (Fig. 12A–D), numerous discrete dissolution pits, of the approximate size and shape of rod-shaped cells,

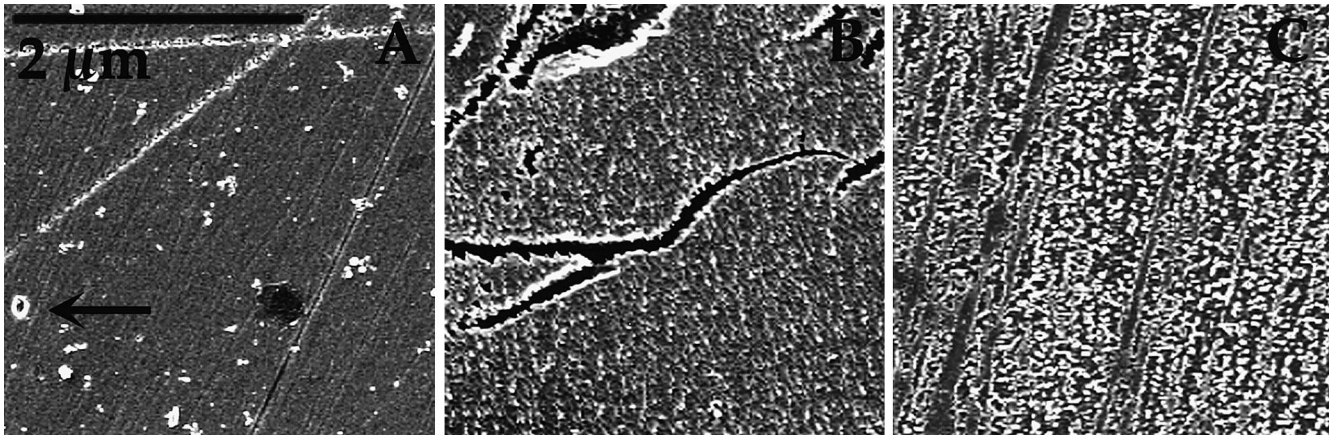

Fig. 11. SEM images of pyrite (A), marcasite (B), and arsenopyrite (C) after abiotic reaction in medium alone at 37°C for 22 days (control samples; no Fe^{3+} or microbial catalyst). Scale bar in A applies to B and C.

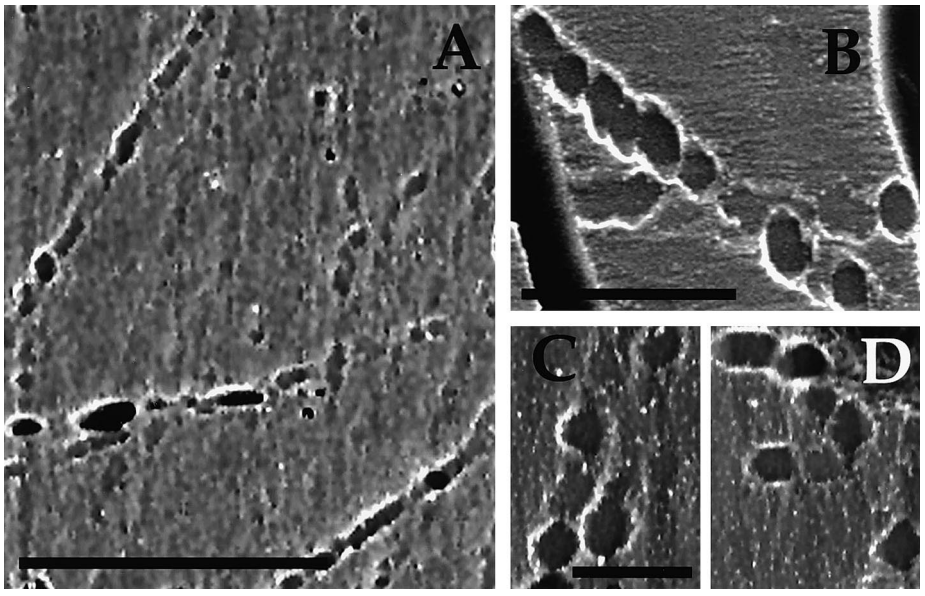

Fig. 12. SEM images of pyrite surfaces reacted abiotically with ferric chloride (at 42°C). Surfaces shown in A (scale = 10 μm), B (scale = 5 μm), C (scale = 2 μm and applies to D) and D were reacted for 3.7 h; numerous cell-sized and cell-shaped pits are evident on these surfaces, similar in size and shape to those seen in Figs. 1 and 8.

were observed on the surface. Some of these developed from the etching of silicate inclusions (not shown). After 28.5 days of reaction (not shown), pit size has increased and the pit shape was more euhedral.

4. Discussion

4.1. Leaching patterns on sulfide minerals

The results of these experiments indicate that pyrite dissolution in the presence of either a microbial or abiotic catalyst takes place via surface roughening and the formation of discrete dissolution pits, which enlarge, aggregate, and become increasingly euhedral over time. Some minor differences may be noted between the microbially reacted surfaces and those reacted abiotically with Fe^{3+} (Fig. 12), most likely due to differences in reaction rates, heterogeneities between mineral samples, or solution chemistries; no reproducible or systematic differences were noted. However, it is clear that cell-sized and -shaped pit formation on pyrite occurs in the presence of Fe^{3+}, irregardless of the presence or absence of microbial cells, and is remarkably similar in either case (Figs. 1, 8 and 12).

Cell-sized and cell-shaped dissolution pits did not form abiotically on pyrite in the absence of Fe^{3+} in our experiments. However, it is well known that pyrite dissolution rates in the absence of Fe^{3+} (abiotic or microbially produced) results in slower overall dissolution rates [17]. Hence, it is likely that in our experiments, surface reactions did not progress far enough over the duration of this study to produce them (Fig. 11). These findings suggest that the formation of cell-sized and cell-shaped dissolution pits does not require a direct microbially induced surface reaction. Additionally, we never observed *A. ferrooxidans* (and *F. acidarmanus*) cells physically located within cell-sized and cell-shaped dissolution pits on pyrite. These observations are consistent with previous SEM reports of *A. ferrooxidans* on pyrite [6–8,15,18]. Other authors that have noted that *A. ferrooxidans* cells were not observed within cell-sized dissolution pits attributed this to detachment and reattachment at a nearby locality [5,6,8]. In order to evaluate this hypothesis, some data on cell residence time are needed. However, it is not possible to estimate cell residence time with any degree of accuracy based on ex situ observations, such as used here and in previous studies [6–8,15,18]. However, in this study, we found that many *A. ferrooxidans* cells resided on surfaces long enough for extensive mineral coverage (Fig. 5) without forming detectable dissolution pits. This suggests that metabolically active *A. ferrooxidans* cells may not reside long enough in one place to produce discernible pits on pyrite (at 25°C), but cannot be conclusive based on the aforementioned nature of ex situ analysis. However, if shallow pits form but are obscured by the cells themselves until detachment, one would predict that similar phenomena (i.e. cell-sized and cell-shaped pitting) would be observed on other sulfide minerals that are known to be capable of supporting growth of the same iron-oxidizing acidophiles, such as marcasite and arsenopyrite. This was clearly not found to be the case in our study. Rather, no bacillus-sized or -shaped dissolution pits were observed on either marcasite or arsenopyrite surfaces at any stage of reaction with *A. ferrooxidans*, substantiating our suspicion that

pit formation on pyrite is intrinsic to the mineral, and not obligatorily linked to the activity of individual cells at the surface.

In our study, only in the case of *F. acidarmanus* reacted with arsenopyrite were cells found partially collapsed within shallow cell-sized and -shaped pits (Fig. 10), suggesting that the dissolution rate at the cell surface was faster than the dissolution rate on the bulk surface (not in contact with cells). It is not certain why cell-induced pitting occurred during reaction with *F. acidarmanus* but not with marcasite or pyrite. However, it is possible that because of the overall increased reactivity of arsenopyrite compared with pyrite and marcasite (by about a factor of two and four, respectively, for these specific minerals [16]), the different total reaction that could occur over the time interval that one cell resided in one place on these minerals produced these differing effects.

4.2. The direct mechanism?

The existence of a 'direct' mechanism for sulfide oxidation has been debated for years (e.g. [4,9,19–22]). Since the first observations of pitting patterns on pyrite surfaces after reaction with *A. ferrooxidans* [5,6], it has been assumed that reaction between cells and the surface was responsible for the observed etching patterns. In this study, we found that the localized activity of individual cells such as *A. ferrooxidans* is not the most important control in pit formation. This is in part inferred by the lack of association between cells and pits over time on pyrite, and is better substantiated by data for experiments with marcasite and arsenopyrite, on which no cell-sized and cell-shaped pits were ever observed, despite their higher reactivity. This is not to preclude that no reaction takes place between *A. ferrooxidans* cells and sulfide surfaces. Based on localized concentrations of surface oxidants, one would predict increased reaction rates in the vicinity of a cell relative to the bulk. Rather, results of this study suggest that the degree to which preferential etching occurs in the vicinity of a cell relative to that in the bulk can probably not always be discerned using SEM.

Additionally, this study has found interactions between iron-oxidizing cells and sulfide surfaces that may not be all the same. *F. acidarmanus* cells produced detectable pits on arsenopyrite surfaces, indicating that the reaction rate at the cell surface was higher than the reaction rate at the bulk surface. Whether this was the result of a 'direct' enzymatic reaction, or an 'indirect' enzymatic reaction is not known because the iron-oxidizing pathway is unknown.

It is notable where we found 'cell-induced' pitting (*F. acidarmanus* on arsenopyrite), the pit size and shape reflected the size and shape of the cell (Fig. 10). This is in contrast to the bacillus-shaped pits that developed on pyrite during reaction with *F. acidarmanus* (Fig. 8B), that we infer were probably not formed as the result of a specific reaction at the cell–mineral interface. Hence, when cells that are not bacillus-shaped attach to and oxidize pyrite, such as '*Leptospirillum*'-like organisms, direct, cell-induced pitting at the cell–mineral interface should result in vibrio- or spirillum-shaped dissolution pits, reflecting the shape of the cell. To our knowledge, there have not been any reports of vibrio- or spirillum-shaped dissolution pits on pyrite surfaces after reaction with '*Leptospirillum*'-like organisms, nor have we observed this phenomenon in our own laboratory experiments with '*L. ferrooxidans*' (unpublished data). Hence, the inference that '*Leptospirillum*'-like organisms are also pit-forming iron-oxidizers is not supported by any laboratory studies we are aware of.

4.3. Summary

This study has found that the oxidative dissolution of pyrite results in discrete dissolution pits on the surface. Our results show that these pits, while approximately cell-sized and -shaped, are often, if not generally, produced by indirect reactions between a cell and the surface to which it is attached. Similar leaching patterns are produced by abiotic reaction with ferric iron, which suggests that a non-specific interaction between surfaces and aqueous ferric iron is an important control on the surface morphology evolution of pyrite during oxidative dissolution. This is not evidence that reaction is not taking place between cells and mineral surfaces. Rather, it is evidence that reaction may not proceed far enough during the residence time of a single cell on the surface to produce pits that are discernible by SEM.

Acknowledgements

The authors thank Tom Gihring and Philip Bond for discussions, and Brian Hess for assistance in mineral preparation. Support for this work was provided by NSF Grant CHE-9521731.

References

[1] Kelly, D.P. and Wood, A.P. (2000) Reclassification of some species of *Thiobacillus* to the newly designated genera *Acidithiobacillus* gen. nov., *Halothiobacillus* gen. nov., and *Thermithiobacillus* gen. nov.. Int. J. Syst. Bacteriol. 50, 511–516.

[2] Norris, P.R. (1990) Acidophilic bacteria and their activity in mineral sulfide oxidation. In: Microbial Mineral Recovery (Erlich, H.L. and Brierley, C., Eds.), pp. 3–27. McGraw-Hill, New York.

[3] Rawlings, D.E., Tributsch, H. and Hansford, G.S. (1999) Reasons why '*Leptospirillum*'-like species rather *Thiobacillus ferrooxidans* are the dominant iron-oxidizing bacteria in many commercial processes for the biooxidation of pyrite and related ores. Microbiology 145, 5–13.

[4] Silverman, M.P. and Ehrlich, H.L. (1964) Microbial formation and degradation of minerals. Adv. Appl. Microbiol. 6, 153–206.

[5] Berry, V.K. and Murr, L.E. (1978) Direct observations of bacteria

and quantitative studies of their catalytic role in the leaching of low-grade copper bearing waste. In: Metallurgical Applications of Biological Leaching and Related Phenomena (Murr, L.R., Torma, A.E. and Torma, J.A. Eds.), Academic Press, New York.
[6] Bennett, J.C. and Tributsch, H. (1978) Bacterial leaching patterns on pyrite crystal surfaces. J. Bacteriol. 134, 310–317.
[7] Mustin, C., De Donato, P. and Berthelin, J. (1992) Quantification of the intragranular porosity formed in bioleaching of pyrite by *Thiobacillus ferrooxidans*. Biotechnol. Bioeng. 39, 1121–1127.
[8] Rodriguez, L.M. and Tributsch, H. (1988) Morphology of bacterial leaching patterns by *Thiobacillus ferrooxidans* on synthetic pyrite. Arch. Microbiol. 149, 401–405.
[9] Sand, W., Gerke, T., Hallmann, R. and Schippers, A. (1995) Sulfur chemistry, biofilm, and the (in)direct attack mechanism – a critical evaluation of bacterial leaching. Appl. Environ. Microbiol. 43, 961–966.
[10] Arredondo, R., Garcia, A. and Jerez, C.A. (1994) Partial removal of lipopolysaccharide for *Thiobacillus ferrooxidans* affects its adhesion to solids. Appl. Environ. Microbiol. 60, 2846–2851.
[11] Lawrence, J.R., Kwong, Y.T.J. and Swerhone, G.D.W. (1997) Colonization and weathering of natural sulfide mineral assemblages by *Thiobacillus ferrooxidans*. Can. J. Microbiol. 43, 178–188.
[12] Schippers, A., Jozsa, P.G. and Sand, W. (1996) Sulfur chemistry in bacterial leaching of pyrite. Appl. Environ. Microbiol. 62, 3424–3431.
[13] Edwards, K.J., Bond, P.L., Gihring, T.M. and Banfield, J.F. (2000) An Archaeal iron-oxidizing extreme acidophile important in acid mine drainage. Science 279, 1796–1799.
[14] Golyshina, O.V. et al. (2000) *Ferroplasma acidiphilum* gen. nov., sp. nov.: an acidophilic, autotrophic, ferrous iron-oxidizing, cell wall-lacking, mesophilic member of *Ferroplasmaceae* fam. nov., comprising a distinct lineage of *Archaea*. Int. J. Syst. Bacteriol. 50, 997–1006.
[15] Edwards, K.J., Schrenk, M.O., Hamers, R. and Banfield, J.F. (1998) Microbial oxidation of pyrite: Experiments using microorganisms from an extreme acidic environment. Am. Mineral. 83, 1444.
[16] Edwards, K.J., Bond, P.L. and Banfield, J.F. (2000) Characteristics of attachment and growth of *Thiobacillus caldus* on sulfide minerals: A chemotactic response to sulfur minerals? Environ. Microbiol. 2, 324–332.
[17] Nordstrom, D.K. and Southham, G. (1997) The geomicrobiology of acid mine drainage. In: Geomicrobiology: Interactions between Microbes and Minerals, Vol. 35 (Banfield, J.F. and Nealson, K.H., Eds.), pp. 361–390. Mineralogical Society of America, Washington, DC.
[18] Mustin, C., Berthelin, J., Marion, P. and De Donato, P. (1992) Corrosion and electrochemical oxidation of a pyrite by *Thiobacillus ferrooxidans*. Appl. Environ. Microbiol. 58, 1175–1182.
[19] Fowler, T.A. and Crundwell, F.K. (1998) Leaching experiments of zinc sulfide by *Thiobacillus ferrooxidans*: Experiments with a controlled redox potential indicate no direct bacterial mechanism. Appl. Environ. Microbiol. 64, 3570–3575.
[20] Groudev, S. (1979) Mechanism of bacterial oxidation of pyrite. Microbiology 16, 75–87.
[21] Larsson, L., Olsson, G., Holst, O. and Karlsson, H.T. (1993) Oxidation of pyrite by *Acidianus brierleyi*: Importance of close contact between the pyrite and the microorganisms. Biotechnol. Lett. 15, 99–104.
[22] Fernandez, M.G., Mustin, C., De Donato, P., Barres, O., Marion, P. and Berthelin, J. (1995) Occurrences at mineral–bacteria interface during oxidation of arsenopyrite by *Thiobacillus ferrooxidans*. Biotechnol. Bioeng. 46, 13–21.